

Early stages of Schottky-barrier formation for Al deposited on GaAs(110)

J. Ortega, F. J. García-Vidal, R. Pérez, R. Rincón, and F. Flores

Departamento de Física de la Materia Condensada C-XII, Facultad de Ciencias, Universidad Autónoma, E-28049 Madrid, Spain

C. Coluzza, F. Gozzo, and G. Margaritondo

Institut de Physique Appliquée, Ecole Polytechnique Fédérale, PH-Ecublens, CH-1015 Lausanne, Switzerland

Y. Hwu, L. Lozzi, and S. La Rosa

Department of Physics, University of Wisconsin, Madison, Wisconsin 53706

(Received 5 February 1992)

Schottky-barrier formation for Al on GaAs(110) was analyzed theoretically and with the aid of synchrotron-radiation photoemission experiments as a function of the metal coverage. For various Al-overlayer thicknesses we calculated the most stable geometries, using a consistent parameter-free linear combination of atomic orbitals method. Our results show that for an Al monolayer, no density of states appears near the semiconductor charge-neutrality level, in agreement with ultrahigh-resolution photoemission spectra. Theory and experiments agree in obtaining a shrinking of the gap. The theory also shows that the Fermi level is pinned, and the Schottky barrier completely formed, for a coverage of two metal monolayers. For this limit we recover the intrinsic-metal-states model and find good agreement with the Schottky-barrier height for thick metal layers. The experiments reveal some complexity in the intermediate-coverage interface-formation process, with the formation of metal clusters beginning at nominal coverages of 2–4 monolayers; this is somewhat unexpected in the present study because of the low substrate temperature.

I. INTRODUCTION

One of the main experimental facts, recently obtained in the study of Schottky-barrier formation, is the evolution of the Schottky-barrier height as a function of the metal coverage deposited on the semiconductor.^{1–3} Typically, for III-V semiconductors, the free surface shows no Fermi-level pinning; the metal deposition introduces a quick evolution on the interface Fermi energy which is eventually pinned by a high density of states induced in the semiconductor gap by one or two metal monolayers. These results have yielded important information on the mechanisms controlling Schottky-barrier formation.

These results have also stimulated theoretical work^{4–6} achieving a better understanding of the chemisorption processes associated with metal deposition on semiconductors, and their relation to the mechanisms of metal-semiconductor interface formation. Much work^{3,6,7} has been recently performed on the deposition of alkali metals on GaAs(110); this is a case that presents some particular advantages, because the metal atoms are very large and do not seem to diffuse into the semiconductor. The Schottky-barrier formation appears to be controlled in this case by a competition between the formation of a conventional conduction band that induces a high density of states in the semiconductor energy gap, and typical electron correlation effects that tend to open a gap inside the metal conduction band (for low metal coverage), thus reducing the density of states induced by the metal in the semiconductor gap.

The aim of the present paper is to analyze the deposition of Al on GaAs(110) in the submonolayer and the

overlayer regimes. Chemisorption properties, Fermi energies, and barrier heights are analyzed as a function of the metal coverage. Our analysis tries to elucidate how the Schottky barrier depends on the Al coverage, compared with the results for the alkali-metal case. We shall discuss the main differences and similarities between these two cases.

We note that the deposition of Al on GaAs is complicated by an exchange reaction whereby Al replaces Ga in the last semiconductor layers. This reaction, which usually proceeds at room temperature, can be expected to be mostly inhibited at the very low temperatures at which the experiments reported here were performed. Our theoretical work assumes that we are in this low-temperature limit, and only considers how Al chemisorbs when it is deposited on the semiconductor. Even with this assumption, the problem is far from being a simple task; we shall analyze different adsorption sites and look for the geometry having the lowest energy.

The theoretical predictions, in particular, as far as the states very near the Fermi level are concerned, were tested by means of synchrotron-radiation photoemission experiments performed at very high energy resolution [Gaussian full width at half maximum (FWHM) of the order of 20 meV]. We found full agreement with a number of significant results, notably the absence of states near the charge-neutrality level for the monolayer-coverage regime, and the shrinking of the gap. The experiments, however, also revealed the formation of clusters and some complexity in the interface morphology for intermediates coverages.

The rest of the paper is organized as follows: in Sec. II

we present a summary of our method of calculation; in Sec. III we discuss our main results. Our experimental tests are described in Sec. IV; finally, in Sec. V we present our main conclusions.

II. MODEL AND METHOD OF CALCULATION

The electronic structure of GaAs is described using a linear combination of atomic orbitals (LCAO) model with sp^3s^* hybrids and the interactions discussed by Vogl, Hjalmarson, and Dow.⁸ The interaction between the Al atoms and between Al and the substrate is analyzed by means of a LCAO method⁹ that gives a prescription to calculate the hopping elements between the different orbitals as well as the one-body and the many-body contributions to the total energy of the chemisorption system. A full discussion of this parameter-free method is presented elsewhere;⁹ here, we only quote its main characteristics. We should mention that parametrizing the semiconductor band structure and using our LCAO method to calculate the metal-semiconductor interaction, instead of using a full LCAO method for the whole system, simplifies the calculation considerably and, also, gives a good description of the bands around the semiconductor energy gap.

First of all, let us mention that the hopping integrals T_{ij} between two orbitals ψ_i and ψ_j (taken as the atomic orbitals of two atoms) are related to the Bardeen tunneling current T_{ij}^B by

$$T_{ij} = \gamma T_{ij}^B, \quad (1)$$

$$T_{ij}^B = \frac{\hbar}{2m} \int (\psi_i \bar{\nabla} \psi_j - \psi_j \bar{\nabla} \psi_i) \bar{n} ds, \quad (2)$$

where γ is typically around 1.3–1.5, a parameter that can be calculated exactly.⁹

The overlap between different orbitals, $S_{ij} = \langle \psi_i | \psi_j \rangle$, introduces a contribution to the total energy that is found to be well described by the following correction to the diagonal level δE_i of a given orbital ψ_i :

$$\delta E_i = - \sum_{j \neq i} S_{ij} T_{ij} + \frac{1}{4} \sum_{j \neq i} S_{ij}^2 (E_i - E_j), \quad (3)$$

where E_i and E_j are the mean levels of the i and j orbitals.

Many-body contributions are introduced by means of the following terms in the total Hamiltonian:

$$\begin{aligned} \hat{H}^{\text{MB}} = & \sum_i U_i^{(0)} \hat{n}_{i\uparrow} \hat{n}_{i\downarrow} + \frac{1}{2} \sum_{i \neq j, \sigma} J_{ij}^{(0)} \hat{n}_{i\sigma} \hat{n}_{j\sigma} \\ & + \frac{1}{2} \sum_{i \neq j, \sigma} \bar{J}_{ij}^{(0)} \hat{n}_{i\sigma} \hat{n}_{j\sigma}, \end{aligned} \quad (4)$$

where $U_i^{(0)}$ and $J_{ij}^{(0)}$ are the intrasite and intersite bare Coulomb interactions, respectively, and $\bar{J}_{ij}^{(0)}$ an effective⁹ intersite Coulomb interaction given by

$$\bar{J}_{ij}^{(0)} = J_{ij}^{(0)} (1 + S_{ij}^2) - J_{x,ij}^{(0)}, \quad (5)$$

where $J_{x,ij}^{(0)}$ is the exchange integral between the i and j orbitals.

The terms given by Eq. (4) are treated using a many-body approximation equivalent to the one given by Slater

for a free electron gas. This means using a mean-field approximation supplemented by a Slater-like potential, $V_{x,i\sigma}$. Thus, we replace Hamiltonian (4) by the following mean-field Hamiltonian:

$$\begin{aligned} \hat{H}_{\text{eff}}^{\text{MB}} = & \sum_i U_i^{(0)} \hat{n}_{i\sigma} \langle \hat{n}_{i\bar{\sigma}} \rangle + \sum_{j \neq i, \sigma} J_{ij}^{(0)} \hat{n}_{i\sigma} \langle \hat{n}_{j\bar{\sigma}} \rangle \\ & + \sum_{j \neq i, \sigma} \bar{J}_{ij}^{(0)} \hat{n}_{i,\sigma} \langle \hat{n}_{j\sigma} \rangle + \sum_{i,\sigma} \alpha V_{x,i\sigma} \hat{n}_{i\sigma} \end{aligned} \quad (6)$$

plus some constant terms canceling the double counting in the electron-electron interaction. $V_{x,i\sigma}$, which is related to the exchange pair distribution function $g_\sigma(i, j)$, is given by

$$V_{x,i\sigma} = - \sum_{j \neq i} \bar{J}_{ij}^{(0)} g_\sigma(i, j), \quad (7)$$

where $g_\sigma(i, j)$ is defined as

$$\langle c_{j\sigma}^\dagger c_{j\sigma} \rangle \langle c_{i\sigma}^\dagger c_{i\sigma} \rangle = \langle \hat{n}_{i\sigma} \rangle g_\sigma(i, j). \quad (8)$$

In Eq. (6), α is taken to be $\frac{7}{4}$: this is shown⁹ to include *interatomic* correlation effects. This implies neglecting *intra-atomic* correlation effects which could be, however, included by using a perturbative approach.¹⁰

In our actual calculation we have solved the LCAO mean-field Hamiltonian using conventional Green-function techniques.¹¹ Moreover, self-consistency in the charges is achieved by relating the induced potential (as given by the many-body Hamiltonian) to the charges induced in each atom. (The induced potential is calculated by means of the intra-atomic, U , and interatomic, J , Coulomb potentials introduced above.)

Let us finally comment that, in general, the semiconductor surface is not allowed to relax. Different theoretical calculations have shown^{12,13} that Al tends to eliminate very efficiently the surface relaxation appearing at a free semiconductor surface. Thus, in all our results, the chemisorption energy of different overlayers are referred relative to the semiconductor unrelaxed surface.

III. RESULTS

We have analyzed the geometries associated with different Al coverages. We have considered three different cases: (A) half a monolayer (ML), (B) a monolayer, and (C) two monolayers. (Here, a ML is defined as 2 Al atoms per semiconductor surface cell.) For each case, we have looked for the most stable geometry.

A. Half a monolayer

Figure 1 shows the two most energetic geometries. In one case, the Al atoms are bonded to As, while in the second case, Al is bonded simultaneously to As and Ga, occupying the midpoint of the largest bridge distance between the cation and the anion. Figure 1 also shows the chemisorption energy for each case, as a function of the distance between the Al layer and the last semiconductor layer. The minimum of the interaction potential yields the following chemisorption energies per adsorbed atom:

$$E_{\text{chem}}(\text{As bonded}) = -1.8 \text{ eV} ,$$

$$E_{\text{chem}}(\text{bridge}) = -2.1 \text{ eV} .$$

We should also mention that, for Al bonded to Ga, we find the following chemisorption energy:

$$E_{\text{chem}}(\text{Ga bonded}) = -1.0 \text{ eV} .$$

B. The monolayer case

In this case we have two Al atoms per surface unit cell. We have explored different geometries and have found

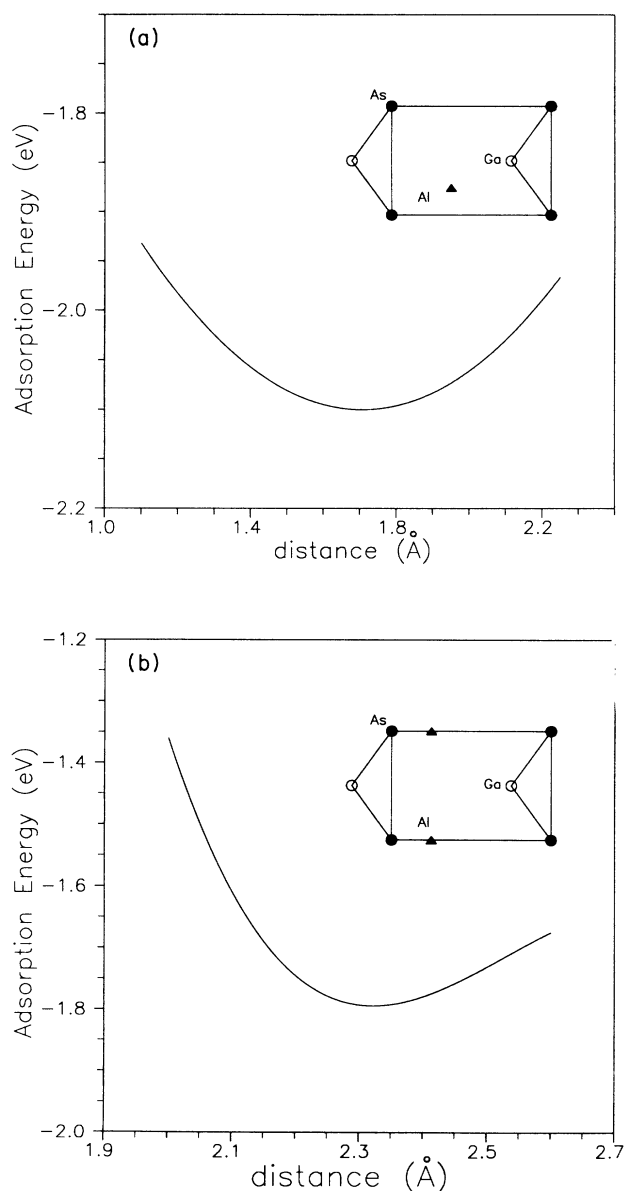


FIG. 1. Chemisorption energy for half a monolayer of Al on GaAs as a function of the metal distance to the last semiconductor layer (in Å). (a) Bridge position. (b) As position. The insets show the corresponding geometries.

that the most favorable geometry corresponds to the case of the Al atoms bonded to the As and Ga dangling bonds (see the inset of Fig. 2). The chemisorption energy for this geometry as a function of the distance between the Al layer and the semiconductor surface is shown in Fig. 3(a). It is interesting to mention that the total chemisorption energy we find for the most stable geometry of the monolayer, $E_{\text{chem}} = -5.3 \text{ eV}$, is larger than the sum of the chemisorption energies calculated independently for the cases of half a monolayer of Al bonded to either As or Ga. This yields 2.8 eV, showing that the Al atoms attract each other tending to form clusters on the GaAs(110) surface. This geometry yields a more favorable geometrical configuration than having two Al atoms chemisorbed on the bridge positions.

In Fig. 3(b) we show the chemisorption energy of the Al monolayer as a function of the distance of one Al atom to the semiconductor surface; here, the other Al atom is placed in the equilibrium position found previously [Fig. 3(a)]. In the most stable geometry, the distance between Al atoms in the Al-Al chains is only 2.45 Å, and this fact would usually imply a repulsive interaction between Al atoms. However, in this case the exchange and correlation contributions to the total energy increase significantly, more than compensating for the repulsive interaction.

Figure 2 also shows the local density of states projected on the two Al atoms and the As and Ga atoms of the last semiconductor layer. We shall comment on these results in the perspective of other theoretical approaches¹² and some experimental evidence.¹⁴ First of all, the results we have already presented for the geometries of half and one monolayers are in good agreement with other results¹²

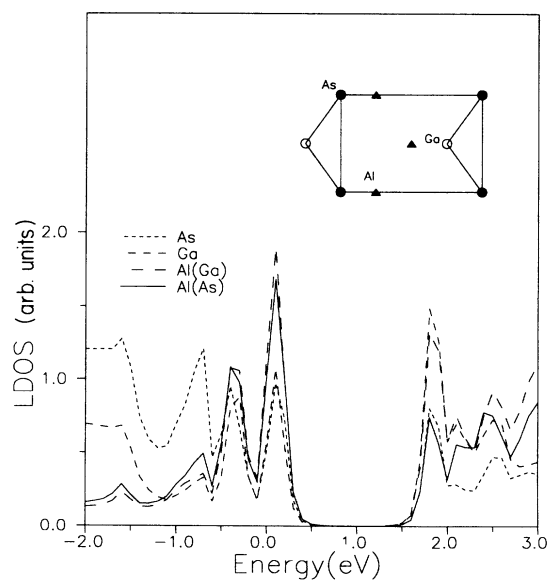


FIG. 2. Local density of states (LDOS) on the metal atoms bonded to Ga and As, and on the cation and the anion of the last semiconductor layer, for the monolayer case shown in the inset. This case corresponds to the most stable Al monolayer geometry. $E = 0$ is the top of the semiconductor valence band.

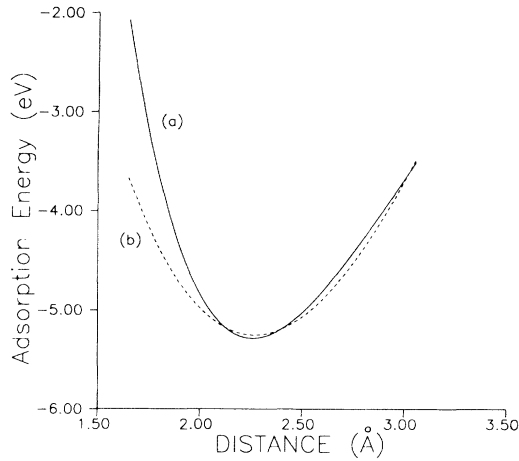


FIG. 3. (a) Chemisorption energy for the monolayer of Al on GaAs shown in the inset of Fig. 2, as a function of the metal distance to the last semiconductor layer (in Å). (b) Chemisorption energy of the Al monolayer as a function of the distance of one Al atom to the semiconductor layer (in Å). The other Al atom is placed on the equilibrium position found in (a).

obtained using a local-density approximation (LDA) method. In particular, the LDA calculation has also obtained the long-bridge position and the Ga and As dangling-bond positions as the most favorable geometries for half monolayer and one monolayer, respectively. (These results differ from those obtained using the simple tight-binding approach of Klepeis and Harrison.¹⁵) This good agreement between the two different theoretical approaches is very gratifying, because recently some experimental scanning tunnel microscopy (STM) results¹⁴ have suggested that Al adsorbed on GaAs should be located on top of Ga. This conclusion is drawn from the different spots that STM images show for positive and negative biases: basically, these images show that for both biases, the brighter spots appear on Ga. In order to see whether these results are compatible with the most stable geometry calculated by the theoretical results, we have shown the different local density of states of an Al monolayer in Fig. 2. The important results one can draw from this figure are the following.

(a) The unoccupied states located just above the energy gap have mainly a Ga character; in particular, the Al bonded to Ga presents also a larger weight in this part of the electronic spectrum.

(b) The occupied states located below the energy gap have as much weight on Ga as on As, if not a little more.

This implies that the local states distributed around the energy gap are mainly of Ga character; thus, these theoretical data seem to explain the STM results, resolving the apparent contradiction between the most stable Al monolayer as calculated here and in Ref. 12, and the STM results.¹⁴ It is also of interest to mention that the density of states shown in Fig. 2 presents an energy gap of around 1.2 eV in good agreement with the value of 1.0 eV obtained by Suzuki and Fukuda¹⁴ using the scanning tunneling microscope.

C. The two-monolayer case

From the point of view of Schottky-barrier formation, one is interested in knowing how the Fermi level is pinned by the electron density of states created in the semiconductor gap. For the monolayer case, we have found that the induced density of states presents an energy gap around 1.2 eV wide. The crucial point is to know how this gap is closed with further deposition of the metal. This has prompted us to analyze the two-monolayer case. Figure 4 shows the geometry of the Al overlayer we have considered; distances between the second Al layer and the other atoms have been calculated by maximizing the chemisorption energy. (This geometry has not been minimized, however, with respect to many other geometrical configurations of the second and first Al layers.¹⁶) The symmetry of the first layer suggests the use of the geometry drawn in Fig. 4, since in this case the new Al atoms are directly bonded to a large number of Al atoms in the first layer. Figure 4 also shows the local density of states that we have calculated for the two-monolayer case, projected onto various metal layers and the last semiconductor layer. The important point to notice is that the interaction introduced by the second Al monolayer *has closed the gap* that appears in the monolayer case. At the same time, we find that the Fermi energy is pinned at 0.6 eV above the semiconductor valence-band top. All these results show good agreement with the behavior of the GaAs(110)/Al interface for low metal coverage, as shown in Sec. IV (see also Ref. 2). For a free semiconductor surface, initially the Fermi level is not pinned by any electron density of states; at very low metal coverage, we expect to have a few islands of monolayer height, and then we should find the electron density of states shown in Fig. 2. Thus the *n*- and *p*-type doped semiconductor Fermi levels at the interface would ap-

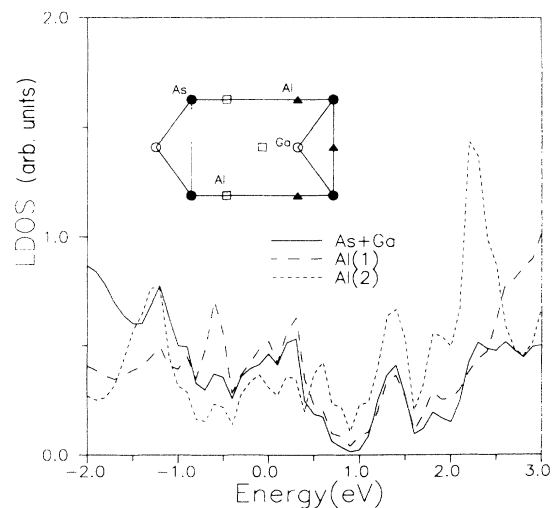


FIG. 4. Local density of states (LDOS) on the two metal layers and the last semiconductor layer for two Al monolayers deposited on GaAs(110). The second Al monolayer is 2.4 Å above the first metal monolayer.

proach each other, but while still differing significantly. Then, for further coverage, Al clusters start to grow, and as soon as a second layer of the cluster is formed, the local Fermi energy is pinned by a high density of states. A macroscopic region will support Fermi-level pinning if the whole surface is covered by Al; this is related, however, to how Al atoms grow on the GaAs surface. What is important to realize is that the Fermi energy given by our calculations for two monolayers should practically coincide with the thick metal overlayer since the barrier height depends only very slightly on the metal coverage,¹⁷ once we have created an important density of states in the semiconductor gap. Now, comparing the position of our calculated Fermi level with the experimental one,² we find quite good agreement, giving further support to the results presented in this paper.

IV. EXPERIMENTAL TESTS

Some of the most relevant predictions of our theoretical treatment were tested with synchrotron-radiation photoemission experiments performed at the Wisconsin Synchrotron Radiation Center. To study metal-semiconductor interfaces the tests required a high energy resolution; such a resolution was originally achieved to investigate the excitation spectrum of high-temperature superconductors,¹⁸ and the general problem of the energy dependence of the broadening in Fermi liquids and potential non-Fermi-liquids.¹⁹ We took advantage of the exceptional characteristics of the instrumentation to perform tests on the GaAs(110)-Al system.

The experimental setup includes the Aladdin storage ring, the 4-m Normal-Incidence Monochromator beamline, a Vacuum Science Workshop high-resolution hemispherical electron spectrometer, and conventional accessory equipment. Careful fine tuning of various parts of the system, in particular, elimination of magnetic fields, enables us to achieve an energy resolution of 20 meV (combined electron and photon analysis, measured as a Gaussian FWHM from the Fermi-edge line shape); in some cases, the resolution was 17 meV. In all cases the high-energy resolution accompanied by a high energy resolution of $\pm 1^\circ$.

The experiments were performed at various angles of photoelectron collection, and the results presented here for normal emission were consistently confirmed by data taken in other directions. Figure 5 shows several high-resolution, normal-emission photoemission spectra taken on in situ cleaved GaAs(110), and then on the same substrate covered by an Al overlayer of increasing nominal thickness.

We note three regimes of the interface formation process: first, a decrease of the GaAs-related signal [curves (b) and (c)], then the formation of metal clusters [curve (d)], and finally the formation of metallic Al [curve (e)]. The first regime is illustrated in detail by Figs. 6 and 7. In Fig. 6 we show the comparison between clean GaAs(110) and the same substrate covered by an overlayer whose nominal thickness is approximately one-third monolayer. In Fig. 7 we show a similar comparison for one monolayer.

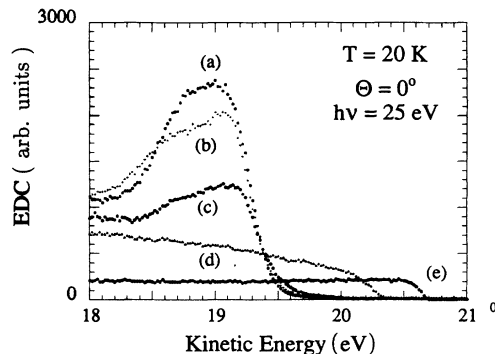


FIG. 5. High-resolution spectra for (a) clean cleaved GaAs(110) taken with a photon energy of 25 eV, in normal emission, at a temperature of 19–20 K, and (b) for the same substrate covered by an Al overlayer with nominal thicknesses of $\frac{1}{3}$ monolayer. Curves (c) and (d) are spectra similar to curve (b) but for normal thicknesses of 1 and 12 monolayers. Curve (e) is for a thick overlayer.

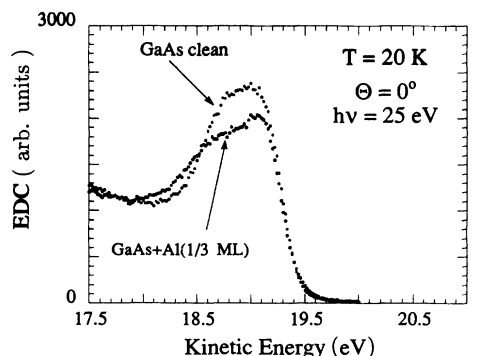


FIG. 6. Direct comparison of the clean-GaAs and the $\frac{1}{3}$ monolayer curves (a) and (b) of Fig. 5, over a more expanded energy scale.

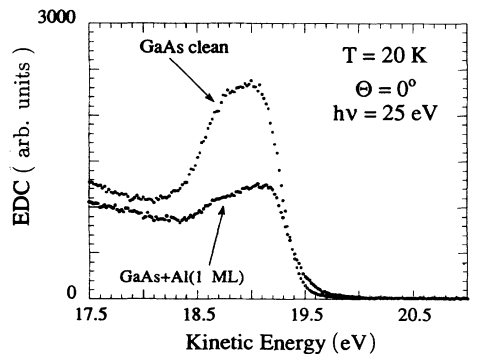


FIG. 7. Comparison similar to that of Fig. 6, involving the one-monolayer curve (c) of Fig. 5.

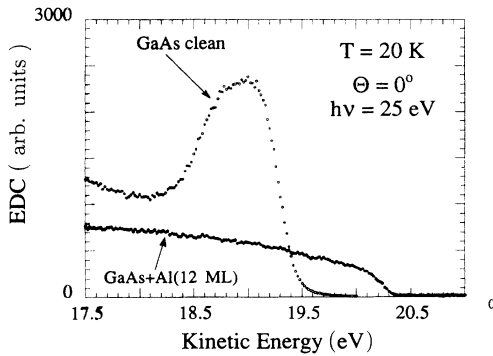


FIG. 8. The formation of metal clusters is revealed by the comparison between curves (a) and (d) of Fig. 5, shown here over a more expanded energy scale.

From Figs. 5–7 we extract two significant points of agreement with the theoretical predictions. First, we see no evidence in this regime of states near the charge-neutrality level. Second, we do observe evidence of a shrinkage of the gap (signal buildup at energies above the clean GaAs edge). This is in agreement not only with the theoretical predictions, but also with the scanning tunnel microscopy (STM) data of Suzuki and Fukuda.¹⁴ Note, however, that our test is not affected by the extreme surface sensitivity of the STM data; thus it can provide a more general confirmation of the gap shrinkage.

For coverages beyond one monolayer, the experiments reveal some complexity in the interface morphology. The most significant finding is the creation of metal clusters. Evidence for this is provided by data like those of Fig. 8 (for 12 monolayers): we see a Fermi edge for the clusters, displaced to lower energy with respect to the Fermi edge of the system. This result is in agreement with earlier room-temperature data, both from photoelectron spectroscopy^{20,21} and STM experiments.¹⁴ In particular, Stoffel, Kelly, and Margaritondo²⁰ used angle-resolved photoemission to analyze the morphology of the cluster-covered surface, finding gallium besides aluminum in the clusters.

The gallium is produced by an exchange reaction, confirmed by the appearance of a free-gallium component in the Ga 3*d* spectrum. Evidence for a weak component

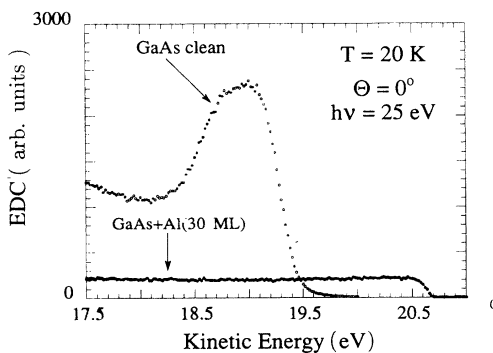


FIG. 9. Comparison of the clean GaAs curve (a) and thick Al curve (e) from Fig. 5.

of this kind was found in our experiments. We note that the formation of clusters at such a low temperature is somewhat surprising, since the surface mobility is reduced, and aluminum should tend to form nearly epitaxial layers.

The latest stage of interface formation, illustrated by Fig. 9, corresponds to the creation of a thick metal overlayer with a well-defined Fermi edge. The edge provides a reference for the conclusion based on Figs. 1 and 2 that no states are created at low coverages near the charge-neutrality level.

V. CONCLUDING REMARKS

The aim of this paper has been to understand Schottky-barrier formation in the case of Al deposition on GaAs(110). It has been established that this barrier formation depends critically on the interaction between the semiconductor and the first metal layers deposited on the surface.^{17,22} These facts have prompted us to analyze the chemisorption energy of the first metal layers deposited on the semiconductor and determine the most favorable geometries. Our results present a good agreement with other theoretical results and have shown to be in agreement with the available experimental evidence. Using the most favorable geometries, we have analyzed Schottky-barrier evolution as a function of coverage. The main conclusion of our analysis is that for an Al monolayer there appears an energy gap around the Fermi energy in the density of states induced by the deposited metal. This explains why, for very low Al coverage, the Fermi level cannot be pinned by the intrinsic states predicted by the induced density of interface states (IDIS) model^{22,23} to appear around the semiconductor charge-neutrality level. Our results also show that for a larger deposition, as soon as a second Al layer is formed (probably, by the formation of Al clusters at the surface), a significant density of states is induced by the metal around the semiconductor charge-neutrality level. Then, the IDIS model becomes applicable, and the interface Fermi level should be located close to that charge-neutrality level. This basically implies that the barrier is completely formed, and that no further evolution of the Schottky barrier and the Fermi level would appear with further metal deposition.

It should be emphasized that this picture of Schottky-barrier evolution is at variance with what has been found for the alkali-metal atoms.^{6,7,24,25} In this latter case, the atoms have a large size and for the first monolayer deposition, only one atom is deposited on the semiconductor per unit cell. Also, the alkali-metal atoms on the semiconductor surface tend to repel one another, and the chemisorption energy, for coverages lower than 1 ML, decreases with increasing coverage. The monolayer case presents a narrow half-filled surface band induced by the adsorbed alkali-metal monolayer, located near the charge-neutrality level of the semiconductor, in which intrasite correlation effects are important.^{7,10} These effects reduce dramatically the electron density of states at the Fermi energy, where a Kondo-like peak is found to pin the Fermi level; also, two other peaks in the local density of states appear below and above the Fermi energy.¹⁰

Further deposition of alkali-metal atoms reduces these effects, and a substantial density of states is finally induced at the Fermi level. For Al on GaAs(110), we find a different case: the semiconductor dangling bonds drive the Al atoms to a geometrical configuration, for the monolayer case, where two metal atoms per unit cell are deposited on the semiconductor. More importantly, that geometry (the natural continuation of the semiconductor surface) implies a kind of surface semiconductor electron structure for the first deposited monolayer. Schottky-barrier formation is, then, related to the closing of this gap due to further deposition of the metal on the semiconductor.

ACKNOWLEDGMENTS

This theoretical work has been partially funded by the Comisión Interministerial de Ciencia y Tecnología (SPAIN) under Contracts Nos. PB-89-0165 and MAT-88-0544, and the CEE under Contract No. SC1-CT 91-0691. The experimental work was supported by the Fonds National Suisse de la Recherche Scientifique, by the Ecole Polytechnique Fédéral de Lausanne, by the Consorzio Interuniversitario Nazionale di Fisica della Materia (INFM), and performed at the Wisconsin Synchrotron Radiation Center, supported by the U.S. National Science Foundation.

-
- ¹K. Stiles, A. Kahn, D. G. Kilday, and G. Margaritondo, *J. Vac. Sci. Technol. B* **5**, 987 (1987); K. Stiles and A. Kahn, *Phys. Rev. Lett.* **60**, 440 (1988).
- ²T. Kendelewicz, P. Soukiassian, M. H. Bahkshi, Z. Hurych, I. Lindau, and W. E. Spicer, *Phys. Rev. B* **38**, 7568 (1988); W. E. Spicer, *Appl. Surf. Sci.* **41-42**, 1 (1989).
- ³M. Prietsch, M. Domke, C. Laubschat, and G. Kaindl, *Phys. Rev. Lett.* **60**, 436 (1988); M. Prietsch, M. Domke, C. Laubschat, T. Mandel, C. Xue, and G. Kaindl, *Z. Phys. B* **74**, 21 (1989).
- ⁴W. Mönch, *Europhys. Lett.* **7**, 275 (1988).
- ⁵I. Lefebvre, M. Lannoo, and G. Allan, *Europhys. Lett.* **10**, 359 (1989).
- ⁶J. Ortega and F. Flores, *Phys. Rev. Lett.* **63**, 2500 (1989); J. Ortega, R. Pérez, and F. Flores, *Surf. Sci.* **251/252**, 442 (1991).
- ⁷T. Maeda Wong, N. J. DiNardo, D. Heskett, and E. W. Plummer, *Phys. Rev. B* **41**, 12 342 (1990); N. J. DiNardo, T. Maeda Wong, and E. W. Plummer, *Phys. Rev. Lett.* **65**, 2177 (1990).
- ⁸P. Vogl, P. Hjalmarsen, and J. D. Dow, *J. Phys. Chem. Solids* **44**, 365 (1983).
- ⁹F. J. Gracia-Vidal, A. Martín-Rodero, F. Flores, J. Ortega, and R. Pérez, *Phys. Rev. B* **44**, 11 412 (1991); E. C. Goldberg, A. Martín-Rodero, R. Monreal, and F. Flores, *ibid.* **39**, 5684 (1989).
- ¹⁰F. Flores and J. Ortega, *Europhys. Lett.* **17**, 619 (1992).
- ¹¹F. Guinea, C. Tejedor, F. Flores, and E. Louis, *Phys. Rev. B* **28**, 4397 (1983).
- ¹²J. Ihm and D. Joannopoulos, *Phys. Rev. B* **26**, 4429 (1982).
- ¹³S. B. Zhang, M. L. Cohen, and S. G. Louie, *Phys. Rev. B* **34**, 768 (1986).
- ¹⁴M. Suzuki and T. Fukuda, *Phys. Rev. B* **44**, 3187 (1991).
- ¹⁵J. E. Klepeis and W. A. Harrison, *Phys. Rev. B* **40**, 5810 (1989).
- ¹⁶In particular, the geometry of the first layer will change as the coordination number increases. However, this geometry is kept unchanged to show how the gap closes with further deposition of Al.
- ¹⁷J. Ortega, J. Sánchez-Dehesa, and F. Flores, *Phys. Rev. B* **37**, 8516 (1988).
- ¹⁸Y. Hwu, L. Lozzi, M. Marsi, S. La Rosa, M. Winokur, P. Davis, M. Onellion, H. Berger, F. Gozzo, F. Lévy, and G. Margaritondo, *Phys. Rev. Lett.* **67**, 2573 (1991).
- ¹⁹Y. Hwu, L. Lozzi, S. La Rosa, M. Onellion, P. Almeras, F. Gozzo, F. Lévy, H. Berger, and G. Margaritondo, *Phys. Rev. B* **45**, 5438 (1992).
- ²⁰N. G. Stoffel, M. K. Kelly, and G. Margaritondo, *Phys. Rev. B* **27**, 6561 (1983).
- ²¹R. R. Daniels, A. D. Katnani, Te-Xiu Zhao, G. Margaritondo, and Alex Zunger, *Phys. Rev. Lett.* **49**, 895 (1982).
- ²²F. Flores and C. Tejedor, *J. Phys. C* **20**, 145 (1987).
- ²³C. Tejedor, F. Flores, and E. Louis, *J. Phys. C* **10**, 2163 (1977); J. Tersoff, *Phys. Rev. Lett.* **30**, 4874 (1984).
- ²⁴J. Ortega, R. Pérez, F. J. García-Vidal, and F. Flores, *Appl. Surf. Sci.* **56-58**, 264 (1992).
- ²⁵J. Hebenstreit, M. Heinemann, and M. Scheffler, *Phys. Rev. Lett.* **67**, 1031 (1991).